



RedirectedDoors+: Door-Opening Redirection with Dynamic Haptics in Room-Scale VR

Downloaded from: <https://research.chalmers.se>, 2025-12-04 23:27 UTC

Citation for the original published paper (version of record):

Hoshikawa, Y., Fujita, K., Takashima, K. et al (2024). RedirectedDoors+: Door-Opening Redirection with Dynamic Haptics in Room-Scale VR. IEEE Transactions on Visualization and Computer Graphics, 30(5): 2276-2286. <http://dx.doi.org/10.1109/TVCG.2024.3372105>

N.B. When citing this work, cite the original published paper.

© 2024 IEEE. Personal use of this material is permitted. Permission from IEEE must be obtained for all other uses, in any current or future media, including reprinting/republishing this material for advertising or promotional purposes, or reuse of any copyrighted component of this work in other works.

RedirectedDoors+: Door-Opening Redirection with Dynamic Haptics in Room-Scale VR

Yukai Hoshikawa , Kazuyuki Fujita , Kazuki Takashima , Morten Fjeld , and Yoshifumi Kitamura 

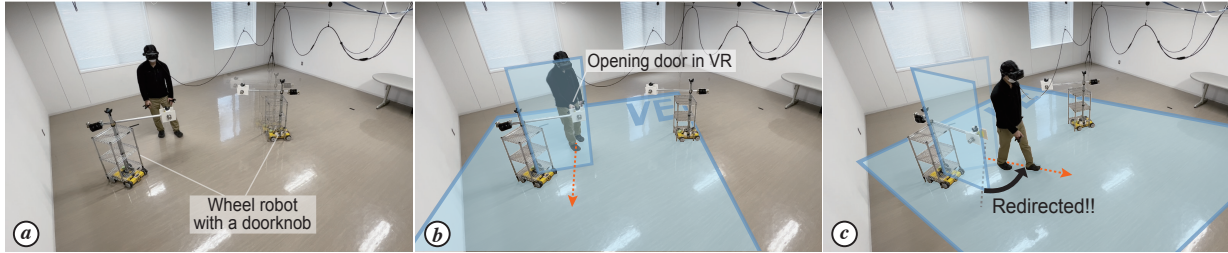


Fig. 1: Overview of RedirectedDoors+. (a) The system provides the user with haptic feedback of opening doors in room-scale VR by adaptively controlling a small number of wheel robots with a doorknob prop. (b-c) During door opening, the system rotates the entire virtual environment by a specific amount, thus steering the user away from the boundary of the play area.

Abstract— RedirectedDoors is a visuo-haptic door-opening redirection technique in VR, and it has shown promise in its ability to efficiently compress the physical space required for a room-scale VR experience. However, its previous implementation has only supported laboratory experiments with a single door opening at a fixed location. To significantly expand this technique for room-scale VR, we have developed *RedirectedDoors+*, a robot-based system that permits consecutive door-opening redirection with haptics. Specifically, our system is mainly achieved with the use of three components: (1) *door robots*, a small number of wheeled robots equipped with a doorknob-like prop, (2) a robot-positioning algorithm that arbitrarily positions the door robots to provide the user with just-in-time haptic feedback during door opening, and (3) a user-steering algorithm that determines the redirection gain for every instance of door opening to keep the user away from the boundary of the play area. Results of simulated VR exploration in six virtual environments reveal our system's performance relative to user walking speed, paths, and number of door robots, from which we derive its usage guidelines. We then conduct a user study ($N = 12$) in which participants experience a walkthrough application using the actual system. The results demonstrate that the system is able to provide haptic feedback while redirecting the user within a limited play area.

Index Terms—Redirected Walking, Visuo-haptic redirection, Encounter-type haptic device, Virtual reality

1 INTRODUCTION

Room-scale virtual reality (VR) provides users with an immersive experience that allows them to explore a virtual environment (VE) by actually walking through it. While this experience can produce a high sense of presence [55] and spatial perception [8], the range of the user's movement is limited by the size of the physical play area. To overcome this limitation, numerous techniques have been explored, including a methodology called redirected walking (RDW) [41], which subtly manipulates the user's movement in VR. However, even with the benefits of these efforts, it is still a challenge to compress the VR experience into a realistic size for use in our homes and offices (e.g., [48]).

At the same time, another major challenge in implementing current VR experiences is that haptic technology is still at a very rudimentary stage, and addressing this has been an active research topic in recent years. In the context of room-scale VR, researchers have studied encounter-type haptic interfaces that can represent the dynamic haptics of VEs using devices such as wheeled robots [13, 32, 52, 59, 64], 2D Cartesian robots [5], or drones [1, 2, 63]. However, these interfaces

were studied in different contexts than the above-mentioned limitations of a physical play area; very few studies [12, 61, 62] have considered combining dynamic haptics with redirection.

RedirectedDoors (RDD) [17, 18], which is a redirection technique focusing on the door-opening motion in VR, is an approach that potentially address both challenges (i.e., limited physical play area and inadequate haptic feedback) simultaneously. This technique subtly manipulates the user's orientation by rotating the entire VE by a specific angular ratio (i.e., gain) of the door being opened by the user. In addition, haptic feedback is provided to the user's hand by a doorknob-like prop during the door opening. The previous report's user study [18] showed that the technique is promising in terms of its high spatial efficiency (i.e., large redirection is possible within a short walking distance of the user) and that the haptic prop contributed to improving the sense of realism and reducing discomfort. Consequently, we believe that deploying this technique will make room-scale VR experiences involving door opening (e.g., exploratory games or simulators for room space design) more effective and richer by reducing the required physical play area while simultaneously providing haptic feedback.

However, one major limitation of previous RDD work [18] is that the implementation only supported the opening of a single fixed door for use in laboratory experiments, and this technique has not yet been applied to more realistic room-scale VR experiences (including consecutive openings of multiple doors in larger VEs). Overcoming this limitation poses two technical challenges. First, while the previous implementation fixed the doorknob haptic prop at a certain location in reality, the haptic prop should be arbitrarily controlled in order to accommodate room-scale VR or to compensate for positional misalignment between reality and VR due to redirection. Second, while the previous work dealt only with user redirection before and after a single door opening, we need a user-steering algorithm to determine the gain

- Yukai Hoshikawa, Kazuyuki Fujita, Kazuki Takashima, and Yoshifumi Kitamura are with Tohoku University. E-mail: yukai.hoshikawa.r4@alumni.tohoku.ac.jp, k-fujita,takashima,kitamura@iec.tohoku.ac.jp.
- Morten Fjeld is with University of Bergen and Chalmers University of Technology. E-mail: Morten.Fjeld@uib.no.

Manuscript received xx xxx. 201x; accepted xx xxx. 201x. Date of Publication xx xxx. 201x; date of current version xx xxx. 201x. For information on obtaining reprints of this article, please send e-mail to: reprints@ieee.org. Digital Object Identifier: xx.xxx/TVCG.201x.xxxxxxx

of redirection during consecutive door openings in order to guide the user and to compress their walking within a smaller play area.

Therefore, in this study we develop **RedirectedDoors+ (RDD+)**, a robot-based system that significantly extends the previous RDD to support room-scale VR experiences involving the successive opening of multiple doors. Specifically, to provide haptic feedback during door opening at arbitrary positions in VR, we implemented a small number of wheeled robots (called **door robots**) equipped with a doorknob-like haptic prop and a **robot-positioning algorithm** to position them at proper timing while avoiding collisions. In addition, to guide the user away from the boundary of the physical play area, we designed and implemented a **user-steering algorithm**, based on existing algorithms [15, 43, 50], that adaptively determines the redirection gain for every instance of door opening. To evaluate the performance of RDD+, we first conducted a simulation study to investigate the effects of VE type, user walking speed, and number of door robots on the spatial efficiency of redirection and robot placement delay. From the results of this simulation, we derived a set of guidelines for realistic use of our system. According to these guidelines, we then implemented a VR walkthrough application using our robot-based system and conducted a user study ($N = 12$). This study demonstrates that our system can simultaneously provide haptic feedback and redirect the user. Furthermore, based on the users' subjective evaluations, we discuss further system improvements and future prospects.

The main contributions of this paper are as follows:

- Engineering and development of an overall RDD+ system that simultaneously supports redirection and haptic presentation of successively opening multiple doors in room-scale VR,
- A set of guidelines for our system derived from a simulation study of VR exploration, and
- Demonstration of an application built upon our actual system and a user study producing insights for further enhancement.

2 RELATED WORK

2.1 Redirected Walking

Redirection is a methodology for overcoming the limitations of a physical play area in room-scale VR by manipulating the user's viewpoint in VR while keeping this manipulation imperceptible by exploiting the dominance of vision over somatosensory perception. In recent years, a vast body of research has been conducted on this topic (see review papers, e.g., [24, 36] for more details). Drawing from these works, here we describe *occasional* redirection techniques (first mentioned by Hoshikawa et al. [18]) and visuo-haptic redirection techniques, which are conceptually aligned with our technique, and then we describe RDD [17, 18], the basis of this study.

2.1.1 Occasional redirection

Occasional redirection refers to the approach of applying visual manipulation occasionally triggered by the user's position or specific actions, in contrast to the conventional approaches like the original RDW [41], where visual manipulation is applied consistently. One way to apply occasional redirection is to explicitly prompt the user to reorient him/herself when approaching the boundary of the play area [45, 60], but this has the limitation of temporarily interrupting the experience due to the reorientation. Another application attempted to integrate the user's reorientation naturally into the narrative of the VR [65], but this may significantly limit the applicable VEs and scenarios.

Another technique is to perform visual manipulation in conjunction with specific user actions or interactions with objects in VR [10, 11, 25, 38, 43, 47]. For example, several studies have exploited inattention blindness [25] and proposed techniques to make redirection less noticeable by placing distracting objects in the VE [38, 47]. Similarly, Schmelter et al. proposed a rotational redirection technique based on bodily interactions (e.g., throwing) in VR games [43]. These interaction-based techniques are advantageous in that they redirect the users without requiring them to walk. However, they are limited in that they require the careful design of interaction targets to match the narrative of the VR experience. Another limitation is that the amount

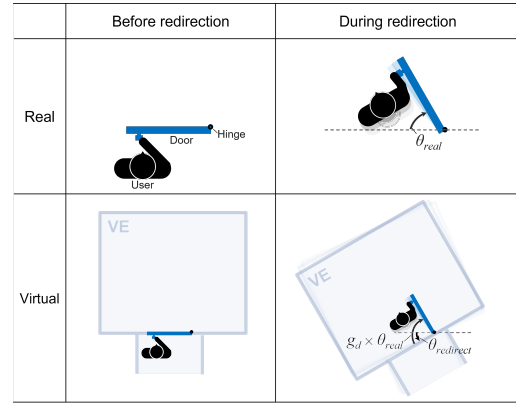


Fig. 2: Overview of RedirectedDoors mechanism [18]

of visual manipulation per interaction is generally small, and repeated interactions are required to achieve user reorientation.

2.1.2 Visuo-haptic redirection

Researchers have explored redirection techniques using visuo-haptic interactions [22, 26–29, 49, 51], which originated with the idea of reusing a single passive haptic prop in RDW [22]. Matsumoto et al. then proposed Unlimited Corridor [27, 29], which allows users to infinitely walk through a corridor in the VE by touching the haptic prop of physical curved walls [27] or handrails [29] based on their findings that haptic cues could make the curvature manipulation less noticeable [26]. Similarly, they proposed Magic Table [28], which provides an illusion of a tabletop shape when touching the haptic prop while walking.

The studies described above are good examples of simultaneously solving the limitations of a physical play area and the lack of haptic feedback. However, in those studies, the haptic props used were fixed to real environments, hindering room-scale VR with varied or dynamic environments.

2.1.3 RedirectedDoors

RDD [18] was the first door-opening redirection technique. This technique redirects the user by rotating the entire VE by a specific angular ratio (i.e., gain g_d) of the door being opened by the user. Figure 2 shows a user opening a door by θ_{real} in reality, thus redirecting the user by $\theta_{redirect}$. Here, the gain g_d is represented as Equation 1.

$$g_d = \frac{\theta_{real} + \theta_{redirect}}{\theta_{real}} \quad (1)$$

The results of their user study suggested a potentially high spatial efficiency of redirection using the technique (i.e., a maximum redirection of 88.8 degrees per door opening without the user noticing it). In addition, they introduced haptic feedback in the doorknob during door-opening redirection using a doorknob-type physical prop. Their user study also showed that the haptic prop was beneficial for improving the sense of presence and reducing the sense of discomfort, while it led to an increased noticeability of the redirection.

An advantage of RDD is that it can be naturally integrated into many VR scenarios because it involves opening doors, which is a frequent action and is related to spatial transition. However, its major limitation is that the previous implementation [18] was only aimed at use in laboratory experiments with an opening of a single fixed door. Their later work [17] introduced a robot-based dynamic haptic presentation system, but it is still an early prototype working only in a single predetermined scenario using a single robot. Therefore, our study aims to develop a system that supports a variety of room-scale VR scenarios including the opening of multiple doors in arbitrary positions.

2.2 Encounter-Type Haptics with Robots

In general, providing appropriate haptic feedback is known to enhance VR immersion [19]. For room-scale VR, however, it is not very practical to install all haptic props that match the VEs [6, 34] or to manually move props [9]. Consequently, researchers have explored encounter-type haptic devices, which adaptively position haptic props according

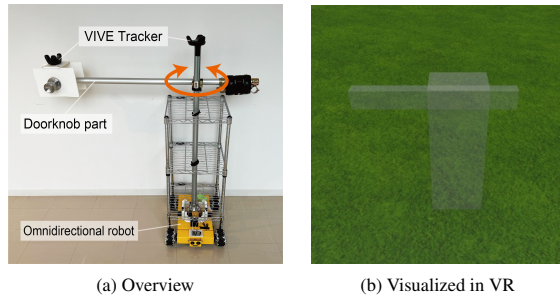


Fig. 3: Door robot

to the user's movements (see review papers, *e.g.*, [31] for more details). Such devices have been developed through various implementations, including wheeled robots [13, 30, 32, 52, 59, 64], 2D Cartesian robots [5], wearable actuators [3, 16, 23, 33, 58], and drones [1, 2, 63]. Here, we describe devices using wheeled robots, which are relevant to this study.

Wheeled robots have often been used for haptic representations of virtual objects fixed in the environment [13, 32, 52, 64]. Examples include furniture-moving robots to reconfigure the physical environment aligned with VE [52] and wheeled robots with vertical surfaces to represent virtual walls [13, 64]. In particular, Yan et al. [64] built a robot control system that deploys haptic props by predicting the user's targeted virtual wall based on the user's walking motion. They mentioned that the device could also be used for doors, and in fact their implementation inspired the one presented in this study.

Despite the various efforts described above, only a few studies [12, 61, 62] have considered combining user redirection with dynamic haptics. Examples include redirection techniques that provide constant haptic cues while walking using a tethered wheeled robot [61] or moving tables [62], but none of them have investigated the haptic cues of opening doors. Therefore, we create new haptic devices and their positioning algorithms for door-opening redirection.

3 REDIRECTEDDOORS+

We developed RedirectedDoors+ (RDD+), a robot-based system enabling consecutive door-opening redirection using dynamic haptics, toward the goal of simultaneously addressing the limitations of a physical play area and the lack of haptic feedback in a variety of room-scale VR scenarios. We believe RDD+ would be particularly compatible with room-scale VR applications involving consecutive door openings, such as indoor exploratory games or interior simulators for space design.

Our system is achieved by adopting the following three components: (1) **Door robots**, a small number of wheeled robots equipped with a doorknob-like haptic prop (described in 3.1), (2) **a robot-positioning algorithm** to correctly position them in real time while avoiding collisions (described in 3.2), and (3) **a user-steering algorithm** that adaptively determines the RDD's gain to keep the user away from the boundaries of the play area (described in 3.3). Figure 4 shows an overview of the implemented RDD+ system workflow.

For the implementation below, we used a PC equipped with an Intel® Core™ i7-9700K CPU @ 3.60 GHz, 16 GB RAM, NVIDIA GeForce RTX 2060 6 GB, Windows 10 Education 64 bit. As for the VR system, we used the Valve Index head-mounted display (HMD), HTC VIVE base stations and controllers, and VIVE trackers. For the software implementation, we used version 2019.4.15 of Unity™ with the SteamVR Plugin.

3.1 Door Robots

To achieve door opening with haptics in room-scale VR, we considered mounting a passive haptic prop on a wheeled robot, as in existing works [13, 37, 52, 59, 64]. This was adopted because it can represent the moving trajectory of a doorknob stably at a relatively low implementation cost.

Figure 3a shows an overview of the implemented door robot. This door robot was newly designed to feature the doorknob prop used in the previous RDD implementation [18] on a wheel robot. We used an omnidirectional mobile robot (Nexus Robot's 4WD 100-mm Mecanum Wheel Robot) because its load capacity was sufficient to carry our

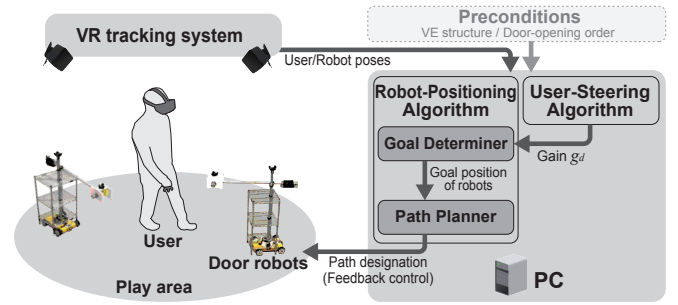


Fig. 4: Overview of RDD+ system workflow

doorknob prop (approx. 6 kg) and its omniwheel locomotion enabled smooth maneuvering. The robot was equipped with a microcontroller (ESP32) and was controlled from a Windows PC through serial communication via Bluetooth. The doorknob-type prop component was connected to a vertical pipe with an orthogonal clamp, which allowed the doorknob to rotate without limitation around the axis of the vertical pipe. In addition, to stabilize the prop on the robot, a metal rack was mounted on the robot via joint parts created by a 3D printer. The force required to push the doorknob was approximately 2.5 N. For tracking the robot in the VR system, we mounted one VIVE tracker at the top of the vertical pipe and another one on the doorknob. These were used to capture the position of the robot itself and the rotation angle of the doorknob. Figure 3b shows how the door robot is visualized in VR, and the reason for the visualization is discussed later in subsection 5.1.

3.2 Robot-Positioning Algorithm

The robot-positioning algorithm allows multiple door robots to work adaptively to provide haptic feedback of the user's door opening. The requirements of the algorithm are to place the robots at the position of the virtual door, to be touched by the user with as little positioning error and delay as possible, and to avoid collisions with the user or other robots while moving within the play area. For our early prototype implementation, we set the assumption that the system knows in advance the structure of the VE (including the number of doors and their locations) and the user's door-opening order in the VE. These assumptions imply that the algorithm cannot support completely free VE exploration with random door openings, but we believe it is still applicable to many unbranched or guidance-based VR scenarios (*e.g.*, tour-type walkthrough applications for viewing of cultural heritage buildings).

As shown in Figure 4, the robot-placing algorithm is achieved by executing two functions: **Goal Determiner**, which determines the destination of each robot as needed to match the position of each door in the VE, and **Path Planner**, which periodically estimates the path to reach the goals while avoiding collisions. To illustrate this algorithm, we present as follows a typical VE consisting of one corridor and three rooms (Figure 5a). In this example, we assume the user visits these three rooms by walking from ③ to ② while passing through three doors (D_1, D_2, D_3) five times in total (respectively identified as $d_1 - d_5$), and the system deploys two door robots (R_1, R_2).

3.2.1 Goal Determiner

Initially, the system assigns a robot to be in charge of each door in the VE. This is simply determined by rotating the robot's ID for each door in order (in the example of Figure 5, the robots in charge of doors D_1, D_2 , and D_3 are respectively determined as R_1, R_2 , and R_1 , as shown in the "Robot in charge" column in Figure 5b). We also considered an alternative strategy of adaptively assigning the robot closest to the designated goal position to be in charge, but we did not adopt this because our informal simulation test showed that simple rotation causes less delay in placement when using three or fewer robots.

Designating the goal position for each robot includes two processes: *approximation* and *fine tuning*. The purpose of the approximation process is to preempt the robot to its likely destination prior to the

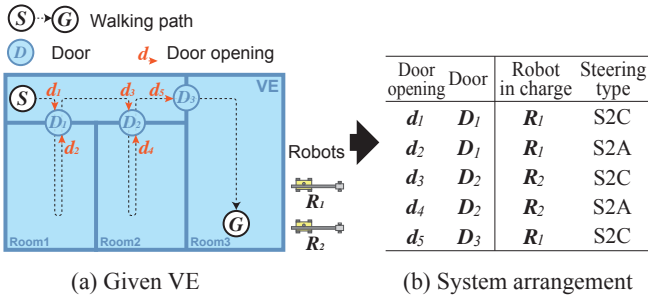


Fig. 5: Example of system arrangements. (a) Given a VE (with three doors) and a user's walking path (with five door openings), (b) the system (with two door robots) determines the robot in charge and the type of steering algorithm used for each door opening (d_i).

user's approach to the door. Specifically, assuming the goal designation of a door D_i , the system sets the destination of D_i to the robot in charge when it detects that the user has finished opening the door D_{i-2} and is headed for the door D_{i-1} (in the example of Figure 5, the destination of door D_3 is designated as robot R_1 at the moment the user finishes opening door D_1). The approximate goal position of D_i is calculated by estimating the redirected angle $\theta_{redirect}$ at the previous door D_{i-1} , which is obtained by the user-steering algorithm described later. Note that the approximate goal position of D_i will necessarily deviate from the true goal, since the actual opening angle θ_{real} at that door D_{i-1} is unknown at the moment of calculation.

The fine tuning process of the goal position is mainly used to compensate for the deviations from the approximation process. During door-opening redirection, the entire VE rotates around the rotation axis (*i.e.*, hinge) of the active door, resulting in a gradually increasing gap between the goal position specified for each robot and the actual position. Therefore, the system updates the goal position every frame (120 Hz) for all of the robots that have a specified goal. This process runs when the system detects any door being opened by users.

3.2.2 Path Planner

For path planning with obstacle avoidance for each door robot, we used the RVO algorithm [57], which has been used in several previous works using wheel robots [37, 52, 64]. The algorithm outputs a provisional path for a robot based on its current position, destination, and the positions of obstacles (*i.e.*, other door robots and the user) as inputs. This calculation is updated for each robot at a frequency of 10 Hz to achieve adaptive path determination in a dynamic environment. For safety, the estimated object size used for RVO collision detection is the actual object size plus a margin. Accordingly, the radius of the door robot is defined as 850 mm, which is somewhat larger than the actual one (810 mm), and the radius of the user is set to 250 mm. A larger margin generally increases safety but at the same time limits the robot's movement range and increases placement delay, so we used a balanced value offering the best compromise based on our preliminary tests.

In addition, we implemented a mechanism to avoid deadlocks caused by path conflicts between robots. This mechanism is triggered in the RVO algorithm when the next robot to be deployed is unable to find a provisional path within a certain period of time (5 s). When triggered, the path for the relevant robot is secured by temporarily changing the destinations of other robots to different locations (away from the path of the relevant robot). Note that deadlocks may also occur when the robot is bounded by the user or the play area's boundaries that limit its movable range; this will be examined in the simulation study below.

For the actual movement control of the door robot based on the determined path, we used PID control. The maximum speed of the robot was limited to 0.40 m/s, which is based on the ISO safety standard [20]. To prevent the robot from unnecessarily vibrating around the goal position when correcting positioning error, we set a positional error tolerance of 20 mm and a rotational error tolerance of 2.5 degrees. With these settings, our informal test confirmed that the user can experience opening doors without any difficulty.

3.2.3 Accuracy Test

We conducted a quick test to examine the basic placement accuracy of the implemented door robot. Using the robot-positioning algorithm described above, we operated one door robot at a random position with 12 different orientations (between 0 and 360 degrees at 20-degree intervals) as destinations in a 5 m \times 5 m space. After each placement, we measured the error of the position and orientation acquired by the VIVE system relative to the destination. We performed this measurement 120 times (12 different angles \times 10 repetitions).

From our results, the mean position error and angular error obtained were 14.5 mm ($SD = 0.43$) and 0.90 deg ($SD = 0.64$), respectively. Although these values may partially include tracking errors of the VIVE system, the placement accuracy of our system is comparable to or better than that of haptic devices using similar wheeled robots [37, 64].

3.3 User-Steering Algorithm

We designed and implemented a user-steering algorithm that adaptively determines the gain of door-opening redirection according to the user's position in reality and the door layout in the VE. The requirement of this algorithm is to redirect the user to restrict walking to as small a real space as possible without this redirection being perceived by them. As with the robot-positioning algorithm, we assume that the system knows in advance the structure of the VE and the user's door-opening order within it.

Based on the above preconditions, we designed an algorithm based on a combination of Steer-to-Center (S2C) [15, 50] and Steer-to-Action (S2A) [43]. S2C is one of the most basic generalized algorithms, and it determines the curvature and/or rotation gain of redirection so that the user's walking direction is toward the center of the play area. S2A is an algorithm based on the locations where specific interactions occur (*i.e.*, action zone); specifically, the amount of redirection (*i.e.*, VE rotation) in the current action zone is determined so that the next action zone is within the play area. Since RDD can be regarded as a kind of interaction-based redirection technique, S2A would generally be suitable. Nevertheless, S2A would not work well alone because it assumes that action zones sequentially exist along the user's walking path in VR, whereas this is not always the case in RDD (*e.g.*, the two successive action zones will be the same if the user moves in and out of one door). Therefore, we considered using either S2A or S2C based on the doors' layout in the VE and their order of opening by the user. In addition, S2C was fine-tuned specifically for our system; since VEs containing multiple doors typically consist of subspaces (*i.e.*, rooms or corridors), we decided to steer the user's current subspace (instead of the entire VE) to be within the play area.

Here, we explain how to determine the steering type (*i.e.*, S2A or S2C) in this algorithm, again using the example in Figure 5. Assuming that the IDs are assigned to the user's opening actions in the order of their passage (d_1 - d_5), the gain applied to a door opening d_i depends on whether the door used for the next door opening d_{i+1} is different from d_i . That is, the system applies S2A if the door used for d_{i+1} is different from that of d_i (*i.e.*, there is another door to be opened next), and it applies S2C if the door used in d_{i+1} is equivalent to d_i or if there is no d_{i+1} (*i.e.*, there is no other door to open). In the example of Figure 5, S2A is applied for the door opening actions d_2 and d_4 where a different door is used next, and S2C is applied for d_1 , d_3 , and d_5 where the same door or no door is used next.

Figure 6 shows an overview of S2A and S2C behaviors, respectively. When S2A is applied at the D_i location, the amount of VE rotation (*i.e.*, $\theta_{redirect}$) is determined so that the direction toward the next door D_{i+1} corresponds to the direction toward the center of the play area (*e.g.*, $\theta_{redirect}$ shown in Figure 6a indicates the determined VE rotation). When S2C is applied at the D_i location, the system tries to incorporate the virtual subspace (*i.e.*, room) entered by opening the door D_i within the play area; the amount of VE rotation is determined so that the direction toward the center of the entered subspace through the door D_i corresponds to the direction toward the center of the play area (*e.g.*, $\theta_{redirect}$ in Figure 6b indicates the determined VE rotation).

Regarding the calculation of the RDD gain (*i.e.*, g_d) to steer the user to the targeted angle $\theta_{redirect}$, the gain cannot be uniquely determined

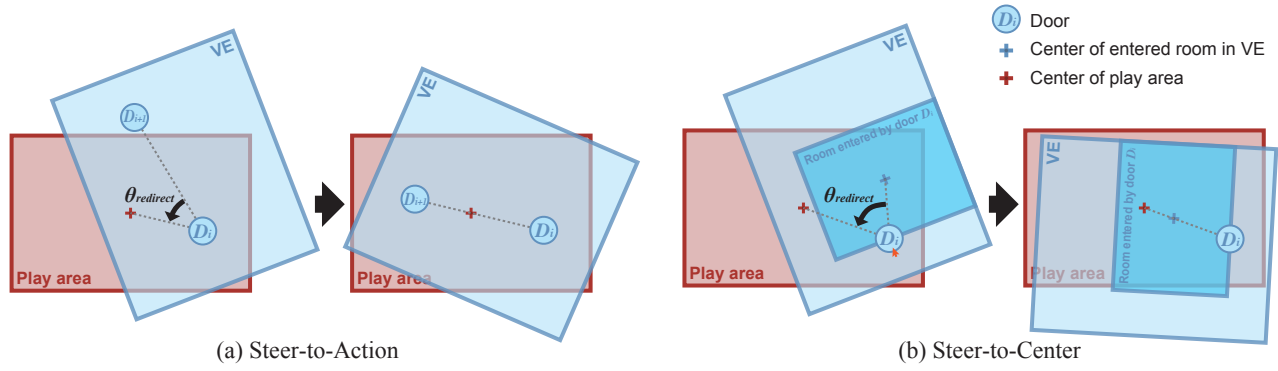


Fig. 6: Behavior of user-steering algorithm at door D_i . (a) Steer-to-Action (S2A) determines the amount of VE rotation ($\theta_{redirect}$) so that the direction toward the next door D_{i+1} corresponds to the direction toward the center of the play area. (b) Steer-to-Center (S2C) determines $\theta_{redirect}$ so that the direction toward the center of the entered subspace through the door D_i corresponds to the direction toward the center of the play area.

since the user's door-opening angle θ_{real} is unknown at the time of calculation. Therefore, we use the regression equation (Equation 2) that estimates the redirected angle $\theta_{redirect}$ as a function of gain g_d , which is obtained from the results of the previous RDD experiment [18]. The actual gain g_d is calculated using Equation 3, which is derived by transforming Equation 2.

$$\theta_{redirect} = a \log_2(g_d) + b \quad (2)$$

$$g_d = 2^{(\theta_{redirect} - b)/a} \quad (3)$$

Here, the parameters a and b (obtained in the previous RDD experiment [18]) are $a = 1.64 \times 10^{-2}$, $b = 7.88 \times 10^{-2}$ when pushing the door and $a = 1.94 \times 10^{-2}$, $b = -1.28 \times 10^{-2}$ when pulling the door.

Then, the final gain value is determined to be within the range of the detection thresholds (between 0.74 and 1.73 for pushing and between 0.49 and 1.48 for pulling [18]) to make the redirection imperceptible to the user. Due to the above gain range, this algorithm alone does not guarantee that the user's walk can be accomplished within a given play area.

4 SIMULATION STUDY

To evaluate the performances of the robot-positioning and user-steering algorithms of RDD+, we conducted a simulation study of a room-scale VR experience. For the robot-positioning algorithm, we investigated how much placement delay, deadlock, and collision occurs while varying the user's walking speed and the number of door robots. For the user-steering algorithm, we investigated the performance of redirection (*i.e.*, how much the physical space required for the VR experience can be compressed) for varied VEs with user walking paths.

4.1 Apparatus

For the simulation, we used the same PC as that used for the implementation. For the software, we used Redirected Walking Toolkit (RDWT) [4], which is often used to simulate RDW, with the addition of RDD+ elements (*e.g.*, the door robots and the door opening redirection).

4.2 Experimental Design

The study had the following three experimental factors: **VE type** (six types: (a) Straight, (b) Spiral, (c) Zigzag, (d) Corridor-left, (e) Corridor-both, (f) Cruciform), **number of door robots** (one, two, three), and **user walking speed** (0.3, 0.6, 0.9 m/s).

The six types of VEs and their corresponding user walking paths (shown in the top area of Figure 7) were determined so that there would be variations in the overall walking path (number, direction, and sequence of turns) and in the positional relationship between successive doors, given the nature of RDD. In addition, we designed three VE types (d, e, f) to include movements in and out of a room through the same door (*i.e.*, where the system applied S2C), which were not involved in the other three VE types (a, b, c), in order to observe the difference in behavior attributable to the steering types of S2A and S2C. The size per room in the VE (3 m \times 3 m) and the width of the

corridor (3 m) were standardized among the VEs. The number of door robots was varied to investigate the impact on placement delay, deadlock, and the risk of collisions with users. A maximum of three robots were used in the simulation as the highest possible number that could be placed comfortably in an ordinary home/office play area. The user walking speed was modified primarily to investigate the robot's placement delay. We set the conditions to cover the maximum user walking speed obtained in previous work (0.87 m/s [64]).

The real play area used in the simulation was 10 m \times 10 m, and the user's initial position in this play area was manually set. We had previously confirmed that the user's walking path for all VE types could fit within this setting using RDD+.

Measurements were taken for redirection performance, robot placement delay (as well as number of deadlocks), and number of collisions. As for redirection performance, we introduced a new metric, **diagonal compression ratio (DCR)**, which indicates how much the user's VE walking trajectory is compressed into a smaller area of real space (due to redirection under the detection thresholds). This ratio is represented by the following equation.

$$DCR = \frac{d_{virtual}}{d_{real}} \quad (4)$$

Here, $d_{virtual}$ and d_{real} are the lengths of the diagonals of the smallest rectangle (*i.e.*, bounding box) containing the user's walking path in VR and in reality, respectively. That is, a smaller DCR indicates that the walking path in reality fits into a smaller space and has higher redirection performance. The reason for using the diagonal instead of the area is to reasonably evaluate the spatial efficiency of redirection, even for some VEs whose areas containing the walking path are calculated to be extremely small (*e.g.*, VE type (a)). Note that DCR does not take into account the robot's path in reality, which needs to be addressed in future work.

The delay time is defined as the time taken for the robot to complete placement at each opening door, relative to when the user arrives at the opening point (manually set approx. 0.5 m in front of each door); the delay time is defined as zero if the robot placement is earlier than the user's arrival and as positive if later. A deadlock is considered to occur when a trial cannot be completed. The number of collisions is defined as the total number of times in a trial that the door robot (W 1150 mm \times D 350 mm, turning radius of doorknob part: 810 mm) comes into contact with the user (radius: 250 mm).

4.3 Procedure

In the simulation software, before the user started walking, a door robot was placed at the first door location designated by Goal Determiner. Then, the user walked from the start point to the goal point at a fixed speed along a predetermined walking path, while the robots moved within the 10 m \times 10 m play area. After arriving at the door, the user waited in a stationary mode if the corresponding door robot was not already in place and then opened the door as soon as that robot was ready. The door opened by the user closed automatically. The door

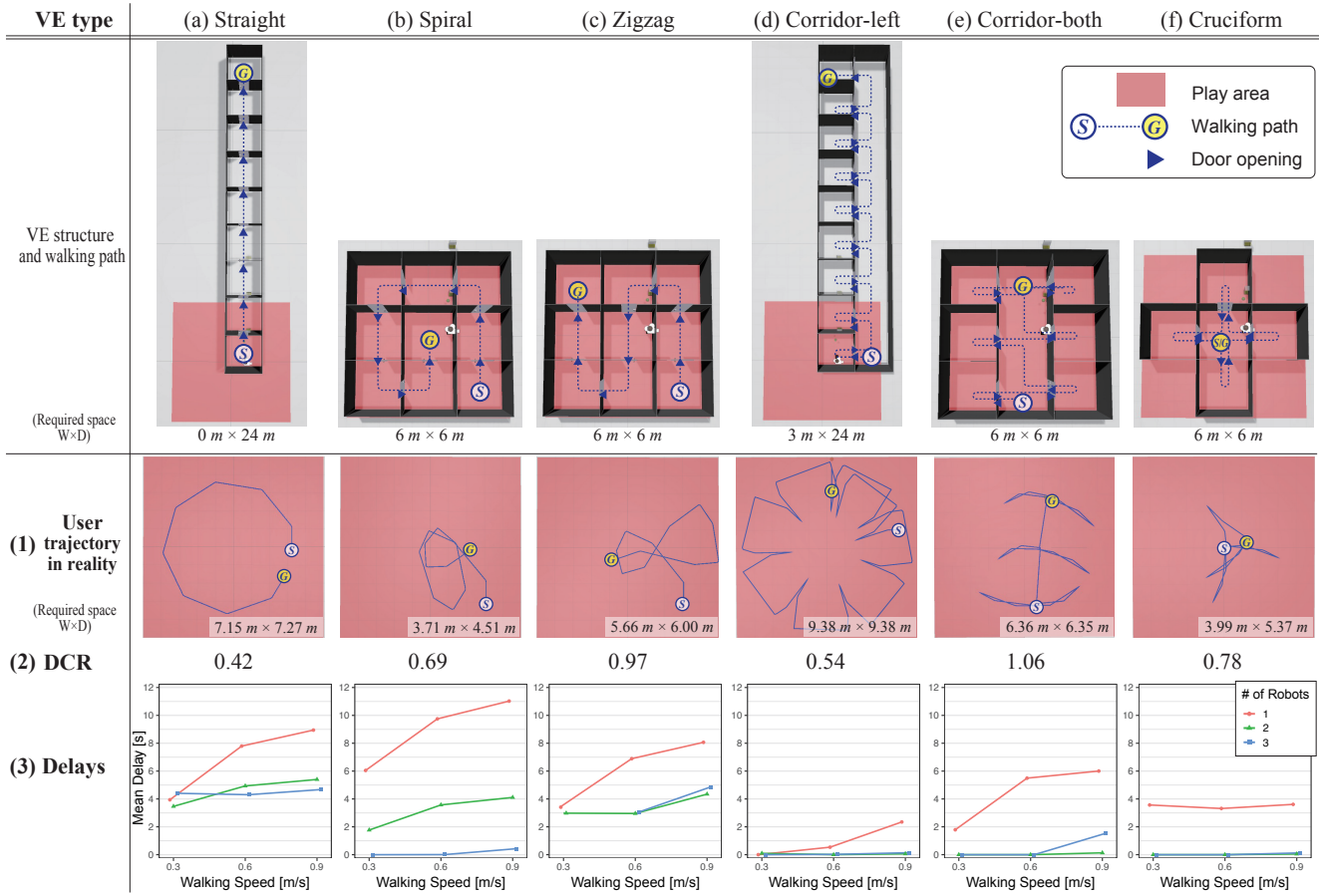


Fig. 7: VE types and corresponding results in simulation study

opening speed in reality was set to the user's average speed (26.5 deg/s) obtained in the previous experiment [18]. The angle for each instance of door opening in reality (*i.e.*, θ_{real}) was calculated from g_d and $\theta_{redirect}$ using Equation 1 and Equation 3. A total of 54 trials were conducted (6 VE types \times 3 numbers of robots \times 3 user walking speeds).

4.4 Results

4.4.1 Redirection Performance

Figure 7(1) shows the tracked user trajectories manipulated by the redirection and Figure 7(2) shows the DCR results in each VE. The mean DCR for all VEs was 0.74 ($SD = 0.22$), which indicates that our algorithm was able to compress the diagonal length of the required real space into 0.74 times that of the VR space. Regarding the DCR results for each VE type, VE type (a) showed the highest compression rate of 0.42, while VE type (e) showed the lowest rate of 1.06. As observed in Figure 7(1), the VEs with high compression rates (*e.g.*, a, b, d) showed circular trajectories, indicating effective use of the real space.

4.4.2 Delays and Deadlocks

Out of 54 trials, one trial (VE type (c), three robots, 0.3 m/s user walking speed) could not be completed due to the deadlock between robots. Aside from this trial, the mean delay time of the robot placement for all trials was 2.83 s ($SD = 2.95$). Figure 7(3) shows the results of the delay time with the number of robots and the user's walking speed for each VE. The graphs show that the delay time generally tends to decrease as the number of door robots increases or as the walking speed decreases. Looking at the differences by VE type, we found that delays were nearly negligible when two or more robots were used in VEs that included in-and-out movements (d, e, f), whereas delays were relatively large in the other VEs, particularly in (a) and (c), where several-second delays were observed even when three robots were used.

The mean delay time for each number of door robots was 5.1 s ($SD = 3.2$) for one, 1.9 s ($SD = 2.0$) for two, and 1.4 s ($SD = 2.0$)

for three. A Wilcoxon signed-rank test with Holm correction between each pair of conditions revealed that the delay time for one robot was significantly longer than those for two and three robots ($p < .01$). The mean delay time for each user walking speed was 1.9 s ($SD = 2.0$) for 0.3 m/s, 2.9 s ($SD = 3.1$) for 0.6 m/s, and 3.7 s ($SD = 3.4$) for 0.9 m/s. Wilcoxon signed-rank test with Holm correction showed no significant difference between each pair of conditions ($p > .05$).

4.4.3 Collisions with User

Out of the 54 trials, collisions with the user occurred a total of 5 times in 4 trials. All of them occurred at a user walking speed of 0.3 m/s, three for VE type (d) (one with two robots and two with three robots), and two for type (e) (one with one robot and one with two robots).

4.5 Discussion

4.5.1 Redirection Performance

The results show that the size of the physical play area required for the experience in the six VEs can be compressed 0.74 times on average in the diagonal. **This demonstrates that our algorithm effectively works to reduce the required play area** in cases where the experience involves a VE with many doors or user movements of opening the same door several times, as used in this study.

The obtained redirection performance depended on the VE type, which was mainly due to the user's walking path between the doors in the VE. For generally straight paths like VE types (a) and (d), the algorithm steered the user's trajectory in a circular manner, showing high redirection performance. As another example, although the two VE types (b) and (c) have similar architectural structures, the DCR results were better for type (b) than for type (c). This was probably due to variations in the direction of turn included in the walking path; type (b) contained four consecutive left turns between doors, which would have worked better with the S2A algorithm than type (c), which contained two left turns and two right turns each. Given the above findings, to

better utilize the redirection of RDD+, **we would recommend that user walking paths between consecutive door openings in a VE be either straight or with turns in the same direction.** Note that this may not be the case depending on the size and shape of the real play area, and further investigation is required.

4.5.2 Delays and Deadlocks

The results show that the delay time varied considerably depending on the VE type. In particular, VEs that included back-and-forth movements through the same door (d, e, f) had smaller delay times than VEs that included only sequential door openings (a, b, c). For example, comparing the delay times in (a) and (d), where the traveling distance of the robots was almost the same, we see that in (a) there was a several-second delay under any condition, while in (d) the delay could be reduced to nearly zero by preparing two or more robots. The reason for this can be attributed to the back-and-forth movements gaining time for the other robots to be deployed at the next door position. Additionally, we observed one robot bypassing the user or another robot in its path of travel in some VEs (e.g., type (c)), which may have been another reason for the increased delay. Thus, the delay might be reduced by adding a mechanism to the RVO algorithm that considers the near-future paths of obstacles that should be moved (*i.e.*, user and other robots).

Nevertheless, eliminating the delay completely using the current setup will be challenging, given that there are other factors that were not considered in the simulation, such as the user's irregular walking path or door-opening angle. One promising solution to this delay is to provide VR narratives to gain time for the robot to deploy. For example, the user-perceived delay could be substantially reduced by adding scenarios to the experience as necessary, such as exploring items of interest, defeating role play enemies, or solving puzzles, and this idea is actually applied in the following user study.

Concerning the number of robots, the results show that the delay time could be reduced by increasing this number, but they also show that the delay time with three robots was not significantly better than that with two robots, while deadlock occurred with three robots. Therefore, **our recommendation is to use two robots, taking into account the increased implementation costs and risk of deadlocks/collisions as the number of robots increases.**

4.5.3 Collisions

Collisions between the user and the door robot were clustered at the lowest user walking speed of 0.3 m/s. In these trials, since the user's speed was comparable to the robot's speed (0.4 m/s maximum), we observed that the robot moved alongside the user, increasing the likelihood of collisions when the robot or user stopped/turned. In particular, collisions in types (d) and (e) occurred probably because the user's walking path included many turns. While collisions at speeds as low as 0.3 m/s are unlikely to cause major problems, finding a comprehensive solution to such collisions may be difficult with the current setup using a somewhat wide doorknob component; collisions could be reduced by increasing the virtual radius of the robot defined in the RVO algorithm, but doing this could also limit the robot's movement range and increase the delays and the risk of deadlocks. Therefore, **we suggest a compromise solution of translucently visualizing the robots in VR so that users themselves can recognize the robots and avoid them**, as considered in several prior encounter-type haptic devices [16, 54, 64].

5 USER STUDY

We conducted a user study to demonstrate the functionality of an actual RDD+ system and to evaluate the user experience with RDD+. For this purpose, according to the results of the simulation study, we implemented a walkthrough application using RDD+. We asked participants to experience this application using three techniques: RDD+, RDD with controllers (RDDwC), and conventional RDW.

5.1 Walkthrough Application with RDD+

Based on the results of the simulation study, we implemented a walkthrough application as a room-scale VR experience compatible with RDD+. In the application, the player opens doors in a predetermined

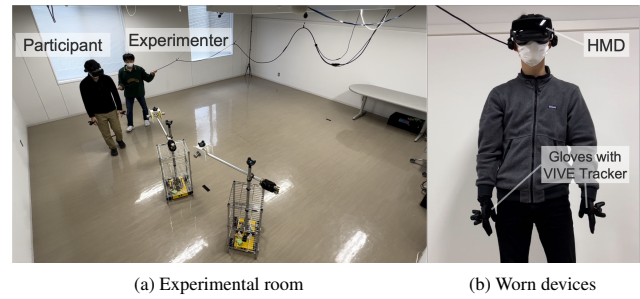


Fig. 8: Experimental setup

order and aims to reach the goal while collecting all needed items, in the manner of an escape game.

We used two types of VEs, indoor and outdoor, as shown in Figure 9. These were respectively scaled down from VE types (b) and (d) in the simulation study, which showed balanced results in redirection performance and robot placement delay. Their sizes were 7.4 m \times 2.5 m for the indoor type and 4.4 m \times 4.2 m for the outdoor type. We prepared two door robots, since this number was found to be cost-effective in the simulation study.

The items that the player had to collect were placed in random positions, one in each room, and could be acquired by the player touching them for three seconds. Such interaction with the items was intended to make the experience less monotonous, while simultaneously gaining time for the door robots to position themselves. When the player opened a door, the door played a creaking sound effect.

We decided to make the door robots visible in VR based on the simulation study results. The position and orientation of the door robot tracked by the VR system were displayed translucently in polygons as shown in Figure 3b. In addition, door panels not ready to be opened (*i.e.*, the corresponding robot is not yet properly positioned) were displayed translucently in VR to allow the user to recognize whether they could be touched.

5.2 Participants

Twelve students (8 males and 4 females, mean age: 22.4, SD=1.00) from a local university participated in the study. Regarding VR experience, one answered "none," three answered "less than five times," and six answered "more than five times." They were paid a reward (about USD 15) for their participation based on the regulations of the university. In the following, we identify them as P1-P12.

5.3 Apparatus

Figure 8a shows the experimental setup. The room size was 5 m \times 5 m and the tracking area was almost identical to it, but the play area was input to the system as 4 m \times 4 m with a margin of 0.5 m from each wall for safety. Because this play area size was smaller than that of the two VEs used, redirection was essential to complete the trials.

We used the same PC and VR system as those used for the implementation. The experimenter held the HMD's cable behind the participant and managed to keep it from tangling with the robot (wire reels attached to the ceiling made it easier to manage the cable). As shown in Figure 8b, participants wore an HMD and gloves with a VIVE Tracker on both hands to visualize the virtual hands in VR. In RDDwC and RDW, they held two VIVE Controllers instead of wearing the gloves.

5.4 Experimental Design

This user study subjectively evaluated room-scale VR experiences with RDD+, compared with using two baseline techniques, RDDwC and RDW. Details of the baseline techniques are given as follows.

- **RedirectedDoors with Controller (RDDwC)** was employed to examine the user experience of RDD without haptic feedback from the robot. Using the method of the previous RDD experiment [18], participants held the controller in both hands and opened the door by moving it while pressing the grip button.
- **Redirected Walking (RDW)** was chosen due to its common nature and also to observe the influence of the qualitative difference

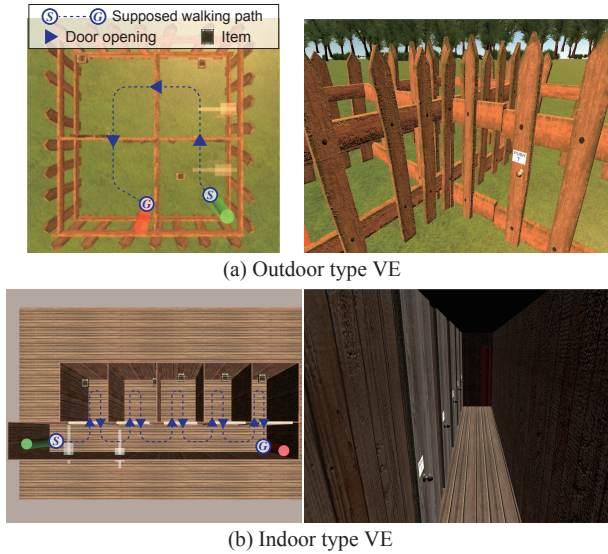


Fig. 9: VEs used in the user study

in redirection on the user experience. RDW was implemented by combining S2C and Reset-to-Center (R2C). For S2C, rotation gain (between 0.8 and 1.49) and curvature gain ($r \geq 7.5m$) were applied based on the previous work [15, 48]. R2C, which has been used in prior work (e.g., [14]), was used when the participant reached the boundary of the play area even with S2C. For R2C, the HMD view displayed “Spin in place,” encouraging users to rotate 360 degrees on the spot and guiding them to orient themselves to the center of the play area by applying the rotation gain. For door opening, a controller-based interface was used, as in RDDwC.

For each technique, one trial was conducted with the two selected VE types, resulting in a total of 3 techniques \times 2 VE types = 6 trials. The reason for not repeating the trial was concern about the participants possibly suffering from simulation sickness by repeating trials.

We obtained sense of presence and simulation sickness as subjective metrics. To evaluate the sense of presence, we used the Slater-Usch-Steed Presence Questionnaire (SUS PQ) [56] for each technique. For simulation sickness, we conducted a Simulator Sickness Questionnaire (SSQ) [21] before and after experiencing each technique. In addition, after experiencing each technique, they were asked to answer a questionnaire about their impressions of the experience and their perception of redirection. The study design of the experiment was officially approved by our university's ethics committee.

5.5 Procedure

The experiment was divided into three main sets, with each set consisting of two trials (including two different VEs) with a specific redirection technique (RDD+, RDDwC, RDW). The order of the presented techniques and VEs was counterbalanced among the participants.

Each set was divided into practice trials and main trials. In the practice trial, the participants practiced opening the door and collecting the items while receiving explanations from the experimenter. During the practice trial, redirection was not applied. The practice trials could be repeated as many times as the participants wished. In the main trial, participants experienced exploration using one of the three techniques; one trial consisted of acquiring items placed in each room in order until finally reaching the goal position. Participants were instructed to open the doors in order as they moved toward the goal (overhead views as in Figure 9 were shown to them before starting the trials) and not to walk too fast for safety (we set a warning to appear in the HMD's view if the walking speed exceeded 1.0 m/s, but this feature was never activated during the main trials). In addition to these instructions in RDD+, we explained the visualization of the robot in VR and instructed users to wait until the robot arrives if the door panel appears translucently in VR. After one trial, the participant's view switched to a VE with only a

Table 1: Results of subjective scores in user study

	RDD+	RDDwC	RDW
SUS PQ	4.74 ($SD = 0.90$)	4.18 ($SD = 1.06$)	4.08 ($SD = 0.91$)
SSQ	11.2 ($SD = 12.8$)	19.3 ($SD = 24.2$)	15.9 ($SD = 19.0$)

marker on the floor, indicating the starting point of the next trial. When the participant arrived at this point, the VE for the next trial was shown.

After each set, participants completed a Google Form questionnaire asking about SUS PQ, SSQ, and qualitative comments about their experience. After the completion of the questionnaire, they took a 5-minute break if they wished, and then moved on to the next set. The entire experiment lasted approx. 60 minutes per participant.

5.6 Results

5.6.1 Execution of RDD+

Of the total of 72 trials, all were completed without problem except for one RDD+ trial that was interrupted. In this trial, a deadlock occurred when the participant unexpectedly stopped for several seconds in the path of a door robot, and the trial resumed after the experimenter manually repositioned the robot. There was no serious collision between a participant and the robots, but it was observed in one trial that a robot made contact with the participant's hand when he was reaching for an item. In addition, two participants (P4, P7) commented that the presence of the robots interfered with their walking progress.

As for the robot placement delays, we examined the number of delays of more than one second as a perceivable length instead of measuring the exact delay time (note: we do not report the duration of delays because of the difficulty in quantitatively determining the exact timing of a user's arrival at a door). Out of the 20 RDD+ trials for 10 participants (excluding P4 and P7, which had missing captured data) from the recorded video, 110 door openings (excluding the first opening of each trial in which no delay could occur) were manually checked, and delays were observed in 24 (21.8 %) of them. The frequency of delays was greater for the indoor type of VE (22 of 90, 24.4 %) than for the outdoor type (2 of 20, 10.0 %).

Regarding redirection applied during the trial, in RDD+ and RDDwC, the participants' walk was contained within the play area in all trials, although the amount of redirection depended on the magnitude of their door-opening angle. In RDW, the participants' walk was kept within the play area only by steering with S2C in 18 out of 24 trials, while in the remaining 6 trials (for five participants), R2C occurred once or twice during the experience.

5.6.2 Sense of Presence

Table 1 shows the obtained SUS PQ scores for each technique. The mean scores were highest for RDD+, followed by RDDwC and RDW. However, a Wilcoxon signed rank test with Holm correction for each of these pairs showed no significant difference between them ($p > .05$).

As for the participants' relevant comments on RDD+, many of them mentioned that the haptic presentation of the door robots enhanced the realism of the door opening and/or the exploration experience (P2, P3, P5, P6, P8, P9, P10, P12). They also raised related feelings such as the fun (P3, P8, P12) and intuitiveness (P9) of door opening and the enhanced sense of movement (P2, P8). However, we also received negative comments on RDD+ regarding its reduced immersive experience due to awareness of the robots (P4, P7, P9, P11, P12), driving noise (P3, P8, P9, P10), waiting time due to placement delay (P3, P5, P9), and misalignment of the doorknob prop (P1, P6).

Regarding RDW, there were few negative comments about S2C. However, many participants who experienced R2C commented that the interruption by it clearly reduced their immersion (P1, P3, P7).

5.6.3 Perception of Redirection

Regarding the visual manipulation by redirection, all 12 participants reported that they noticed it in RDD+ and RDDwC, while only two reported they noticed it (other than R2C) in RDW.

Table 1 shows the obtained SSQ scores for each technique. The mean scores were higher for RDDwC, RDW, and RDD+, in that order, but a Wilcoxon signed rank test with Holm correction on each of the pairs

showed no significant difference between them ($p > .05$). Regarding the participants' comments on sickness, some said that RDD+ and RDDwC were most likely to cause sickness (P8, P11), while others stated that RDW caused sickness the most (P6, P7). The circumstances in which participants felt discomfort in RDD+ were diverse, with opinions such as when pulling (rather than pushing) a door (P2, P8, P10), during the indoor VE (P2, P6, P10, P11) and the outdoor VE (P1), and when opening a door too quickly (P8).

5.7 Discussion

5.7.1 Performance of RDD+ with Actual System

Our application using the actual RDD+ system with two robots successfully performed as expected in most trials, **demonstrating that the system could achieve room-scale VR with both haptic feedback presentation and redirection**. In particular, many participants appreciated the realism of the door-opening experience offered by the haptic feedback of RDD+, which may have resulted in the highest presence score of the three techniques.

However, subjective comments also highlighted the degradation of the user's sense of immersion caused by the robots' behavior, as also suggested in previous encounter-type haptic devices [64]; participants were somewhat aware of the robots' presence in reality through cues such as the robots' placement delay, driving sound, and visualized polygons. This is probably the main reason why, despite the many positive responses to RDD+, its presence score was not significantly better than that of the other two techniques without haptic feedback. Below we discuss possible improvements to the system in more detail.

Robot placement. The application was supposed to mostly resolve the robot placement delay by requiring the user to spend time acquiring items, but the results showed that such delay still occurred. In particular, when comparing the two VE types, the indoor VE (in common with type (b) in the simulation study) showed more frequent placement delays than the outdoor VE (in common with type (e)), contrary to the results of the simulation study. This may be due to the individual differences in the actual door-opening angle, causing the large error in the approximation process in Goal Determiner (please refer to 3.2.1). Particularly in the indoor VE, the fine-tuning process (to compensate for this error) could not have been made in time because no items for gaining time were located in the corridor (*i.e.*, between leaving each room and entering the next room). To improve this, the opening angle for each user could be individually learned over trials to increase the accuracy of the approximation process in Goal Determiner, which could save time for the subsequent fine-tuning process. Another consideration is that redirection with our system could be used to reduce the robot placement delay (*i.e.*, by steering the user through redirection so that the robot can be in place at the right time), as in previous work [12].

In addition, contact with the participant and deadlock were observed in a few trials. To overcome these issues, the algorithm might need to be improved to adaptively predict the possibility of future collisions or deadlocks with the robot based on the user's walking path, in addition to the doors' layout and the order of opening them.

Robot visualization in VR. Visualization of the robot with translucent polygons was a necessary part of our system for safety, but it might be one reason for increasing awareness of the robot and thus reducing the participants' immersion. In fact, while one participant (P3) advocated the need for visualization, others (P4, P9) commented that this detracted from the immersive experience. To address this concern, we would like to apply a more *diegetic* [42] visualization that avoids lowering immersion by replacing robots with objects according to the narratives in the VR, such as monsters or cleaning robots, by following prior efforts [46, 53].

Sound from robots. The sound produced by the robot was a factor in reducing the immersion. This sound was caused by motor operation as well as slippage between the omniwheel and the floor, and thus it could be lowered considerably by using floors with high friction, such as carpets. Another option is for the user to wear noise-canceling headphones or earplugs.

5.7.2 User Perceptions of Redirection

In RDD+ and RDDwC, all participants noticed redirection, even though the gains were within the detection thresholds. There are three potential explanations for this observed effect. The first is that participants' individual detection thresholds simply differed from the one used in this study. The second is the difference in door opening speed. That is, compared to the average door opening speed in the previous RDD experiment (26.5 deg/s) [18], the speed in this study was more than two times higher (59.7 deg/s), which may have helped participants notice the VE rotation more easily. Since this experiment included consecutive door-opening actions, it is possible that the task became more monotonous as the trial progressed, resulting in a larger door-opening speed. The third potential explanation for noticing redirection is that the gains presented to the participants varied with every door opening. For example, in the indoor VE, a gain greater than 1 was used when pushing a door to enter a room, while another gain less than 1 was used when pulling the same door to exit the room. These effect observed is yet to be fully understood and therefore needs to be investigated in the future studies.

6 CONCLUSION, LIMITATIONS, AND FUTURE WORK

In this study, we developed a robot-based system called Redirected-Doors+ (RDD+), which provides consecutive door-opening redirection with haptics in room-scale VR. The results of a simulation study derived guidelines for realistic usage of RDD+ offering higher redirection performance and lower placement delay of the robots. A user study using an RDD+ application confirmed the successful execution of our actual system while redirecting the user within a limited play area. Subjective comments also highlighted the realism of door opening enhanced by the haptic feedback, although some suggestions for improving robot operation emerged. From these results, we conclude that our system simultaneously enables the haptic presentation of opening doors and compression of the required play area through redirection.

One major limitation of this study is that the order of opening doors were fixed. In future work, we will implement real-time prediction of the door that the user will touch next, based on user walking motion, by referring to ZoomWalls [64].

A second limitation is that this study only assumed the use of RDD+ alone. Our simulation study used somewhat specific VE conditions that require many doors to be opened; using our system alone may not be realistic in most VEs where few doors exist. Therefore, future work is to integrate RDD+ with the existing RDW system.

A third limitation is that the current user-steering algorithm focuses only on the relationship between two consecutive doors. Considering the entire layout for all doors may further increase the compression of the required play area. Furthermore, it would be promising to integrate our user-steering algorithm with existing highly advanced algorithms using probabilistic locomotion prediction [35, 67] or automatic graph extraction of VEs [66] to make redirection more intelligent.

A fourth limitation is the small and somewhat biased sample of the user study. For example, gender is known to affect navigation ability [7] and low-level perception [44], and that biased participant pools can lead to biased results [39, 40]. Thus, a more in-depth study with a larger number and diversity of participants would be needed.

The last limitation is the uniformity of the haptic feedback used for door opening in this study. Several improvements to the robot could be considered in order to create diverse door opening experiences, such as instantly switchable doorknob props (cylindrical knob, handle, flat plate, etc.), variable doorknob rotation radii, and variable perceived weight of the doorknob.

ACKNOWLEDGMENTS

This work was supported in part by JSPS Grants KAKENHI (19KK0258, 21H03473), by the Wallenberg Foundations (MMW/MAW), and by the Norwegian Research Council (MediaFutures, 309339).

REFERENCES

- [1] M. Abdullah, M. Kim, W. Hassan, Y. Kuroda, and S. Jeon. Hapticdrone: An encountered-type kinesthetic haptic interface with controllable force feedback: Example of stiffness and weight rendering. In *Proc. IEEE Haptics Symposium*, pp. 334–339, 2018. doi: 10.1109/HAPTICS.2018.8357197 1, 3
- [2] P. Abtahi, B. Landry, J. J. Yang, M. Pavone, S. Follmer, and J. A. Landay. Beyond the force: Using quadcopters to appropriate objects and the environment for haptics in virtual reality. In *Proc. CHI*, p. 1–13. Association for Computing Machinery, New York, NY, USA, 2019. doi: 10.1145/3290605.3300589 1, 3
- [3] A. Achberger, F. Aust, D. Pohlandt, K. Vidackovic, and M. Sedlmair. Strive: String-based force feedback for automotive engineering. In *Proc. UIST*, p. 841–853. Association for Computing Machinery, New York, NY, USA, 2021. doi: 10.1145/3472749.3474790 3
- [4] M. Azmandian, T. Grechkin, M. Bolas, and E. Suma. The redirected walking toolkit: a unified development platform for exploring large virtual environments. In *Proc. WEVR*, pp. 9–14, 2016. doi: 10.1109/WEVR.2016.7859537 5
- [5] E. Bouzbib, G. Bailly, S. Haliyo, and P. Frey. Covr: A large-scale force-feedback robotic interface for non-deterministic scenarios in vr. In *Proc. UIST*, pp. 209–222. Association for Computing Machinery, 2020. doi: 10.1145/3379337.3415891 1, 3
- [6] F. Brooks. What's real about virtual reality? *IEEE Computer Graphics and Applications*, 19(6):16–27, 1999. doi: 10.1109/38.799723 2
- [7] L. Castelli, L. Latini Corazzini, and G. C. Geminiani. Spatial navigation in large-scale virtual environments: Gender differences in survey tasks. *Computers in Human Behavior*, 24(4):1643–1667, 2008. Including the Special Issue: Integration of Human Factors in Networked Computing. doi: 10.1016/j.chb.2007.06.005 9
- [8] S. S. Chance, F. Gaunet, A. C. Beall, and J. M. Loomis. Locomotion mode affects the updating of objects encountered during travel: The contribution of vestibular and proprioceptive inputs to path integration. *Presence*, 7(2):168–178, 1998. doi: 10.1162/105474698565659 1
- [9] L.-P. Cheng, T. Roumen, H. Rantzsch, S. Köhler, P. Schmidt, R. Kovacs, J. Jasper, J. Kemper, and P. Baudisch. Turkdeck: Physical virtual reality based on people. In *Proc. UIST*, p. 417–426. Association for Computing Machinery, New York, NY, USA, 2015. doi: 10.1145/2807442.2807463 2
- [10] C.-B. Ciumedean, C. Patras, M. Cibulskis, N. Váradi, and N. C. Nilsson. Mission impossible spaces: Using challenge-based distractors to reduce noticeability of self-overlapping virtual architecture. In *Proc. SUI*. Association for Computing Machinery, 2020. doi: 10.1145/3385959.3418453 2
- [11] R. Cools and A. L. Simeone. Investigating the effect of distractor interactivity for redirected walking in virtual reality. In *Proc. SUI*. Association for Computing Machinery, 2019. doi: 10.1145/3357251.3357580 2
- [12] E. J. Gonzalez, P. Abtahi, and S. Follmer. Reach+: Extending the reachability of encountered-type haptics devices through dynamic redirection in vr. In *Proc. UIST*, p. 236–248. Association for Computing Machinery, New York, NY, USA, 2020. doi: 10.1145/3379337.3415870 1, 3, 9
- [13] Z. He, F. Zhu, and K. Perlin. Physshare: Sharing physical interaction in virtual reality. In *Proc. UIST*, p. 17–19. Association for Computing Machinery, New York, NY, USA, 2017. doi: 10.1145/3131785.3131795 1, 3
- [14] C. Hirt, Y. Kompis, C. Holz, and A. Kunz. The chaotic behavior of redirection – revisiting simulations in redirected walking. In *Proc. 3DUI*, pp. 524–533, 2022. doi: 10.1109/VR51125.2022.00072 8
- [15] E. Hodgson and E. Bachmann. Comparing four approaches to generalized redirected walking: Simulation and live user data. *IEEE transactions on visualization and computer graphics*, 19(4):634–643, 2013. 2, 4, 8
- [16] A. Horie, M. Y. Saraiji, Z. Kashino, and M. Inami. Encounteredlimbs: A room-scale encountered-type haptic presentation using wearable robotic arms. In *Proc. IEEE VR*, pp. 260–269, 2021. doi: 10.1109/VR50410.2021.00048 3, 7
- [17] Y. Hoshikawa, K. Fujita, K. Takashima, M. Fjeld, and Y. Kitamura. Demonstration of redirecteddoors: Manipulating user's orientation while opening doors in virtual reality. In *Proc. SIGGRAPH Asia XR*. Association for Computing Machinery, New York, NY, USA, 2022. doi: 10.1145/3550472.3558405 1, 2
- [18] Y. Hoshikawa, K. Fujita, K. Takashima, M. Fjeld, and Y. Kitamura. Redirecteddoors: Redirection while opening doors in virtual reality. In *Proc. IEEE VR*, pp. 464–473. IEEE, 2022. doi: 10.1109/VR51125.2022.00066 1, 2, 3, 5, 6, 7, 9
- [19] B. E. Insko, M. Meehan, M. Whitton, and F. Brooks. *Passive haptics significantly enhances virtual environments*. PhD thesis, University of North Carolina at Chapel Hill, 2001. 2
- [20] ISO. Iso/ts 15066:2016(en) robots and robotic devices — collaborative robots, 2016. <https://www.iso.org/obp/ui/#iso:std:62996:en:4>
- [21] R. S. Kennedy, N. E. Lane, K. S. Berbaum, and M. G. Lilienthal. Simulator sickness questionnaire: An enhanced method for quantifying simulator sickness. *The international journal of aviation psychology*, 3(3):203–220, 1993. 8
- [22] L. Kohli, E. Burns, D. Miller, and H. Fuchs. Combining passive haptics with redirected walking. In *Proc. ICAT*, pp. 253–254. Association for Computing Machinery, 2005. doi: 10.1145/1152399.1152451 2
- [23] P. Kudry and M. Cohen. Prototype of a wearable force-feedback mechanism for free-range immersive experience. In *Proc. RACS*, p. 178–184. Association for Computing Machinery, New York, NY, USA, 2022. doi: 10.1145/3538641.3561507 3
- [24] Y.-J. Li, F. Steinicke, and M. Wang. A comprehensive review of redirected walking techniques: Taxonomy, methods, and future directions. *Journal of Computer Science and Technology*, 37(3):561–583, 2022. doi: 10.1007/s11390-022-2266-7 2
- [25] A. Mack. Inattention blindness: Looking without seeing. *Current Directions in Psychological Science*, 12(5):180–184, 2003. 2
- [26] K. Matsumoto, Y. Ban, T. Narumi, T. Tanikawa, and M. Hirose. Curvature manipulation techniques in redirection using haptic cues. In *Proc. 3DUI*, pp. 105–108. IEEE, 2016. doi: 10.1109/3DUI.2016.7460038 2
- [27] K. Matsumoto, Y. Ban, T. Narumi, Y. Yanase, T. Tanikawa, and M. Hirose. Unlimited corridor: Redirected walking techniques using visuo haptic interaction. In *Proc. SIGGRAPH Emerging Technologies*. Association for Computing Machinery, 2016. doi: 10.1145/2929464.2929482 2
- [28] K. Matsumoto, T. Hashimoto, J. Mizutani, H. Yonahara, R. Nagao, T. Narumi, T. Tanikawa, and M. Hirose. Magic table: Deformable props using visuo haptic redirection. In *Proc. SIGGRAPH Asia Emerging Technologies*, pp. 1–2. Association for Computing Machinery, 2017. doi: 10.1145/3132818.3132821 2
- [29] K. Matsumoto, T. Narumi, Y. Ban, Y. Yanase, T. Tanikawa, and M. Hirose. Unlimited corridor: A visuo-haptic redirection system. In *Proc. VRCAI*, pp. 1–9. Association for Computing Machinery, 2019. 2
- [30] L. A. Mendez S., H. Y. Ng, Z. Y. Lim, Y.-J. Lu, and P.-H. Han. Movable-bag: Substitutional robot for enhancing immersive boxing training with encountered-type haptic. In *Proc. SIGGRAPH Asia XR*. Association for Computing Machinery, New York, NY, USA, 2022. doi: 10.1145/3550472.3558406 3
- [31] V. R. Mercado, M. Marchal, and A. Lécuyer. “haptics on-demand”: A survey on encountered-type haptic displays. *IEEE Transactions on Haptics*, 14(3):449–464, 2021. doi: 10.1109/TOH.2021.3061150 3
- [32] S. Mortezaipoor, K. Vasylevska, E. Vonach, and H. Kaufmann. CoboDeck: A Large-Scale haptic VR system using a collaborative mobile robot. In *Proc. IEEE VR*. IEEE, 2023. 1, 3
- [33] K. Nagai, S. Tanoue, K. Akahane, and M. Sato. Wearable 6-dof wrist haptic device “spidar-w”. In *Proc. SIGGRAPH Asia Haptic Media And Contents Design*. Association for Computing Machinery, New York, NY, USA, 2015. doi: 10.1145/2818384.2818403 3
- [34] M. P. R. S. T. B. Néstor Andrés Arteaga Martín, Victor Mittelstädt. Passive haptic feedback for manual assembly simulation. In *Proc. CIRP CMS*, pp. 509–514, 2013. 2
- [35] T. Nescher, Y.-Y. Huang, and A. Kunz. Planning redirection techniques for optimal free walking experience using model predictive control. In *Proc. 3DUI*, pp. 111–118, 2014. doi: 10.1109/3DUI.2014.6798851 9
- [36] N. C. Nilsson, T. Peck, G. Bruder, E. Hodgson, S. Serafin, M. Whitton, F. Steinicke, and E. S. Rosenberg. 15 years of research on redirected walking in immersive virtual environments. *IEEE Computer Graphics and Applications*, 38(2):44–56, 2018. doi: 10.1109/MCG.2018.111125628 2
- [37] Y. Onishi, K. Takashima, S. Higashiyama, K. Fujita, and Y. Kitamura. Waddlewalls: Room-scale interactive partitioning system using a swarm of robotic partitions. In *Proc. UIST*. Association for Computing Machinery, New York, NY, USA, 2022. doi: 10.1145/3526113.3545615 3, 4
- [38] T. C. Peck, H. Fuchs, and M. C. Whitton. Evaluation of reorientation techniques and distractors for walking in large virtual environments. *IEEE Transactions on Visualization and Computer Graphics*, 15(3):383–394, 2009. doi: 10.1109/TVCG.2008.191 2
- [39] T. C. Peck, K. A. McMullen, and J. Quarles. Divrsify: Break the cycle

- and develop vr for everyone. *IEEE Computer Graphics and Applications*, 41(6):133–142, 2021. doi: [10.1109/MCG.2021.3113455](https://doi.org/10.1109/MCG.2021.3113455) 9
- [40] T. C. Peck, L. E. Sockol, and S. M. Hancock. Mind the gap: The underrepresentation of female participants and authors in virtual reality research. *IEEE Transactions on Visualization and Computer Graphics*, 26(5):1945–1954, 2020. doi: [10.1109/TVCG.2020.2973498](https://doi.org/10.1109/TVCG.2020.2973498) 9
- [41] S. Razzaque, Z. Kohn, and M. C. Whitton. Redirected Walking. In *Proc. Eurographics*, pp. 289–294, 2001. 1, 2
- [42] P. Salomoni, C. Prandi, M. Rocchetti, L. Casanova, and L. Marchetti. Assessing the efficacy of a diegetic game interface with oculus rift. In *Proc. IEEE CCNC*, pp. 387–392, 2016. doi: [10.1109/CCNC.2016.7444811](https://doi.org/10.1109/CCNC.2016.7444811) 9
- [43] T. Schmelter, L. Hernadi, M. A. Störmer, F. Steinicke, and K. Hildebrand. Interaction based redirected walking. In *Proc. CGIT*, pp. 1–16. Association for Computing Machinery, 2021. doi: [10.1145/3451264](https://doi.org/10.1145/3451264) 2, 4
- [44] A. Shaqiri, M. Roinishvili, L. Grzeczowski, E. Chkonia, K. Pilz, C. Mohr, A. Brand, M. Kunchulia, and M. H. Herzog. Sex-related differences in vision are heterogeneous. *Scientific reports*, 8(1):7521, 2018. doi: [10.1038/s41598-018-25298-9](https://doi.org/10.1038/s41598-018-25298-9) 9
- [45] A. L. Simeone, N. C. Nilsson, A. Zenner, M. Speicher, and F. Daiber. The space bender: Supporting natural walking via overt manipulation of the virtual environment. In *Proc. 3DUI*, pp. 598–606. IEEE, 2020. doi: [10.1109/VR46266.2020.00082](https://doi.org/10.1109/VR46266.2020.00082) 2
- [46] A. L. Simeone, E. Velloso, and H. Gellersen. Substitutional reality: Using the physical environment to design virtual reality experiences. In *Proc. CHI*, p. 3307–3316. Association for Computing Machinery, New York, NY, USA, 2015. doi: [10.1145/2702123.2702389](https://doi.org/10.1145/2702123.2702389) 9
- [47] M. Sra, X. Xu, A. Mottelson, and P. Maes. Vmotion: Designing a seamless walking experience in vr. In *Proc. DISC*, pp. 59–70. Association for Computing Machinery, 2018. doi: [10.1145/3196709.3196792](https://doi.org/10.1145/3196709.3196792) 2
- [48] F. Steinicke, G. Bruder, J. Jerald, H. Frenz, and M. Lappe. Estimation of detection thresholds for redirected walking techniques. *IEEE Transactions on Visualization and Computer Graphics*, 16(1):17–27, 2010. doi: [10.1109/TVCG.2009.62](https://doi.org/10.1109/TVCG.2009.62) 1, 8
- [49] F. Steinicke, G. Bruder, L. Kohli, J. Jerald, and K. Hinrichs. Taxonomy and implementation of redirection techniques for ubiquitous passive haptic feedback. In *Proc. CW*, pp. 217–223, 2008. doi: [10.1109/CW.2008.53](https://doi.org/10.1109/CW.2008.53) 2
- [50] F. Steinicke, G. Bruder, T. Ropinski, and K. Hinrichs. Moving towards generally applicable redirected walking. In *Proc. IEEE VR*, pp. 15–24. IEEE Press, 2008. 2, 4
- [51] E. A. Suma, D. M. Krum, and M. T. Bolas. Redirection on mixed reality walking surfaces. In *IEEE VR Workshops*, pp. 33–35. IEEE, 2011. 2
- [52] R. Suzuki, H. Hedayati, C. Zheng, J. L. Bohn, D. Szafir, E. Y.-L. Do, M. D. Gross, and D. Leithinger. Roomshift: Room-scale dynamic haptics for vr with furniture-moving swarm robots. In *Proc. CHI*, pp. 1–11. Association for Computing Machinery, 2020. doi: [10.1145/3313831.3376523](https://doi.org/10.1145/3313831.3376523) 1, 3, 4
- [53] Y. Tao and P. Lopes. Integrating real-world distractions into virtual reality. In *Proc. UIST*. Association for Computing Machinery, New York, NY, USA, 2022. doi: [10.1145/3526113.3545682](https://doi.org/10.1145/3526113.3545682) 9
- [54] S.-Y. Teng, C.-L. Lin, C.-h. Chiang, T.-S. Kuo, L. Chan, D.-Y. Huang, and B.-Y. Chen. Tilepop: Tile-type pop-up prop for virtual reality. In *Proc. UIST*, p. 639–649. Association for Computing Machinery, New York, NY, USA, 2019. doi: [10.1145/3332165.3347958](https://doi.org/10.1145/3332165.3347958) 7
- [55] M. Usuh, K. Arthur, M. C. Whitton, R. Bastos, A. Steed, M. Slater, and F. P. Brooks. Walking >Walking-in-Place>Flying, in Virtual Environments. In *Proc. CGIT*, pp. 359–364. Association for Computing Machinery, 1999. doi: [10.1145/311535.311589](https://doi.org/10.1145/311535.311589) 1
- [56] M. Usuh, E. Catena, S. Arman, and M. Slater. Using presence questionnaires in reality. *Presence*, 9(5):497–503, 2000. doi: [10.1162/105474600566989](https://doi.org/10.1162/105474600566989) 8
- [57] J. van den Berg, M. Lin, and D. Manocha. Reciprocal velocity obstacles for real-time multi-agent navigation. In *Proc. IEEE Robotics and Automation*, pp. 1928–1935, 2008. doi: [10.1109/ROBOT.2008.4543489](https://doi.org/10.1109/ROBOT.2008.4543489) 4
- [58] C.-H. Wang, C.-Y. Hsieh, N.-H. Yu, A. Bianchi, and L. Chan. Haptic-sphere: Physical support to enable precision touch interaction in mobile mixed-reality. In *Proc. 3DUI*, pp. 331–339, 2019. doi: [10.1109/VR.2019.8798255](https://doi.org/10.1109/VR.2019.8798255) 3
- [59] Y. Wang, Z. T. Chen, H. Li, Z. Cao, H. Luo, T. Zhang, K. Ou, J. Raiti, C. Yu, S. Patel, and Y. Shi. Movevr: Enabling multiforce feedback in virtual reality using household cleaning robot. In *Proc. CHI*, p. 1–12. Association for Computing Machinery, New York, NY, USA, 2020. doi: [10.1145/3313831.3376286](https://doi.org/10.1145/3313831.3376286) 1, 3
- [60] B. Williams, G. Narasimham, B. Rump, T. P. McNamara, T. H. Carr, J. Rieser, and B. Bodenheimer. Exploring large virtual environments with an hmd when physical space is limited. In *Proc. APGV*, pp. 41–48. Association for Computing Machinery, 2007. doi: [10.1145/1272582.1272590](https://doi.org/10.1145/1272582.1272590) 2
- [61] N. L. Williams, N. Rewkowski, J. Li, and M. C. Lin. A framework for active haptic guidance using robotic haptic proxies. In *2023 IEEE International Conference on Robotics and Automation (ICRA)*, pp. 12478–12485, 2023. doi: [10.1109/ICRA48891.2023.10160996](https://doi.org/10.1109/ICRA48891.2023.10160996) 1, 3
- [62] A. Yamaguchi, S. Yokoi, K. Matsumoto, and T. Narumi. Tablemorph: Haptic experience with movable tables and redirection. In *SIGGRAPH Asia 2023 Emerging Technologies*, SA '23. Association for Computing Machinery, New York, NY, USA, 2023. doi: [10.1145/3610541.3614574](https://doi.org/10.1145/3610541.3614574) 1, 3
- [63] K. Yamaguchi, G. Kato, Y. Kuroda, K. Kiyokawa, and H. Takemura. A non-grounded and encountered-type haptic display using a drone. In *Proc. SUI*, p. 43–46. Association for Computing Machinery, New York, NY, USA, 2016. doi: [10.1145/2983310.2985746](https://doi.org/10.1145/2983310.2985746) 1, 3
- [64] Y. Yixian, K. Takashima, A. Tang, T. Tanno, K. Fujita, and Y. Kitamura. Zoomwalls: Dynamic walls that simulate haptic infrastructure for room-scale vr world. In *Proc. UIST*, pp. 223–235. Association for Computing Machinery, 2020. doi: [10.1145/3379337.3415859](https://doi.org/10.1145/3379337.3415859) 1, 3, 4, 5, 7, 9
- [65] R. Yu, W. S. Lages, M. Nabiyouni, B. Ray, N. Kondur, V. Chandrashekar, and D. A. Bowman. Bookshelf and bird: Enabling real walking in large vr spaces through cell-based redirection. In *Proc. 3DUI*, pp. 116–119. IEEE, 2017. doi: [10.1109/3DUI.2017.7893327](https://doi.org/10.1109/3DUI.2017.7893327) 2
- [66] M. Zank and A. Kunz. Optimized graph extraction and locomotion prediction for redirected walking. In *Proc. 3DUI*, pp. 120–129, 2017. doi: [10.1109/3DUI.2017.7893328](https://doi.org/10.1109/3DUI.2017.7893328) 9
- [67] M. A. Zmuda, J. L. Wonser, E. R. Bachmann, and E. Hodgson. Optimizing constrained-environment redirected walking instructions using search techniques. *IEEE Transactions on Visualization and Computer Graphics*, 19(11):1872–1884, 2013. doi: [10.1109/TVCG.2013.88](https://doi.org/10.1109/TVCG.2013.88) 9